

Supplemental Materials

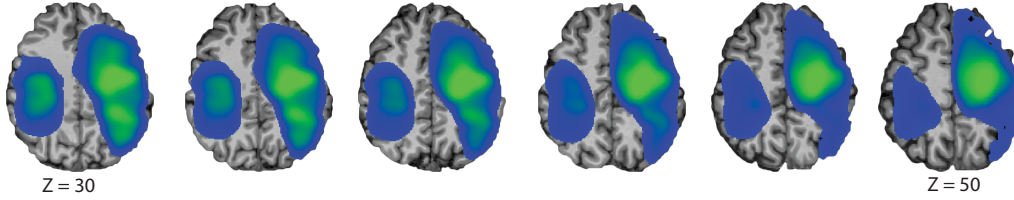
Domain-specific diaschisis: Lesions to parietal action areas modulate neural responses to tools in the ventral stream

Frank E. Garcea, Jorge Almeida, Maxwell H. Sims, Andrew Nunno, Steven Meyers, Michael Li,
Kevin Walter, Webster H. Pilcher, & Bradford Z. Mahon *

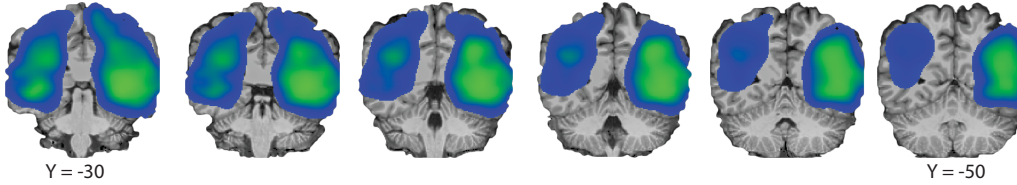
*Author to whom correspondence should be addressed.
Email: mahon@rcbi.rochester.edu

Supplemental Figure 1. Lesion distribution in neurosurgery patients

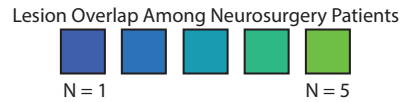
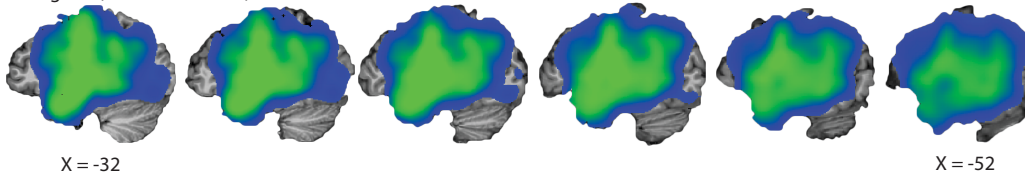
A. Axial (inferior-to-superior)



B. Coronal (anterior-to-posterior)



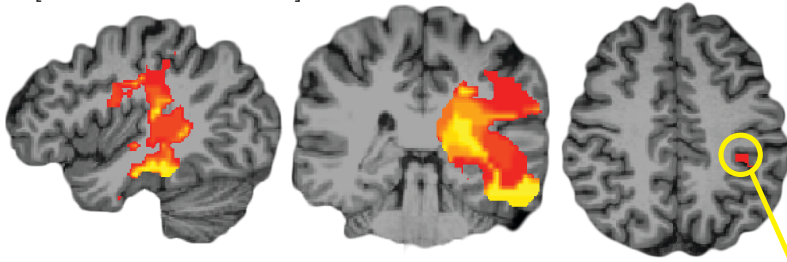
C. Sagittal (medial-to-lateral)



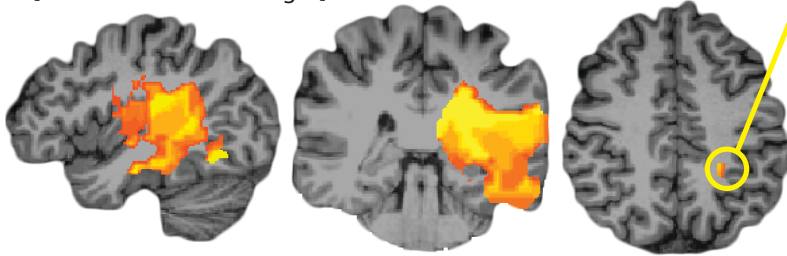
Supplemental Figure 1. Lesion distribution in neurosurgery patients. Voxel lesion overlap among the 35 neurosurgery patients. Lesions were identified using a high-resolution T1 dataset collected during each patient's first pre-operative fMRI scanning session. There is maximal overlap in the left anterior temporal lobe (and adjacent white matter voxels), in left frontal-motor cortex, and in the left anterior and inferior parietal lobe (and in adjacent white matter voxels inferior to the left inferior parietal lobule). Note that the lesion map is presented in radiological convention.

Supplemental Figure 2. The association of aIPS lesions with tool responses in ventral temporal cortex does not depend on the baseline.

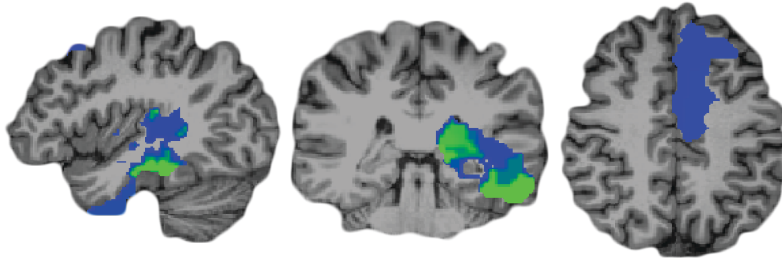
A. [Tools > Animals & Faces]



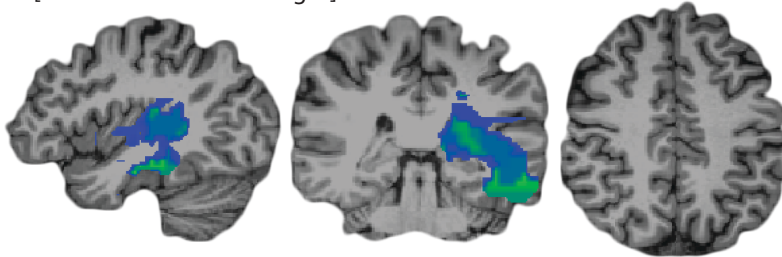
B. [Tools > Scrambled Images]



C. [Places > Animals & Faces]



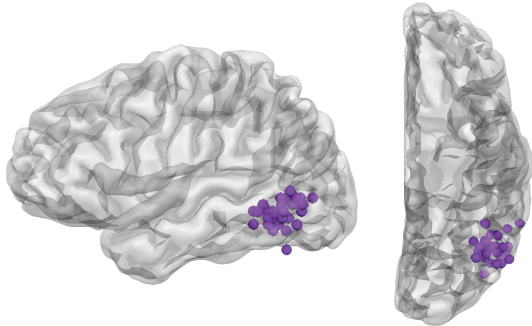
D. [Places > Scrambled Images]



Supplemental Figure 2. The association of aIPS lesions with tool responses in ventral temporal cortex does not depend on the baseline used to calculate tool-preferences in ventral temporal cortex (**Panels A and B**). Lesions to structures in the left anterior and medial temporal lobe and the white matter medial to the left middle and superior temporal gyri are associated with weaker responses to tools (**A-B**) and places (**C-D**) in left ventral temporal cortex. Importantly, aIPS is not identified regardless of the baseline used for calculating place-preferences. All maps set to a minimum threshold of $r(33) = -0.33$, $p < .05$, uncorrected, and cluster-corrected using built-in BrainVoyager software (Alpha-sim, 1000 iterations). Note that the VLAM maps are presented in radiological convention.

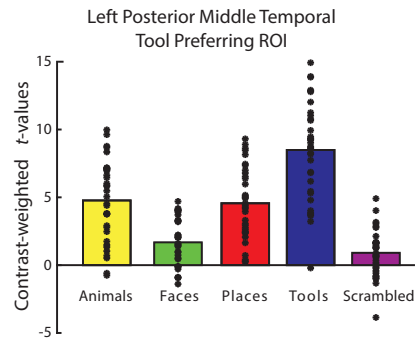
Supplemental Figure 3. Voxel-based Lesion Activity Mapping (VLAM) demonstrates that lesions to aIPS modulate neural responses to tools in the left posterior middle temporal gyrus.

A. Left posterior middle temporal gyrus ROIs for Tool Preferences in the Neurosurgery Group.



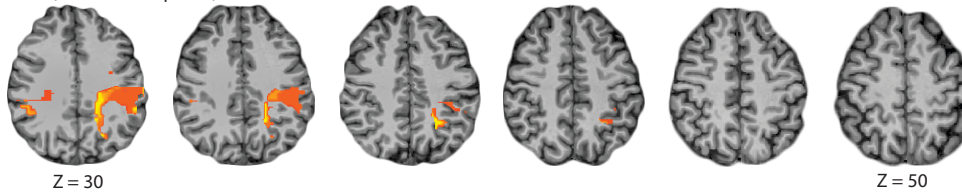
● Individual Subject Left Posterior Middle Temporal Tool Preferring ROI

B. Category Responses in the Neurosurgery Group.

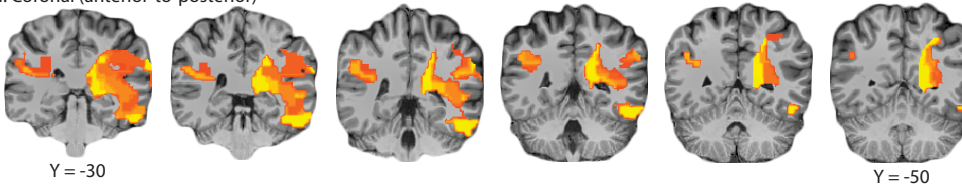


C. Voxelwise correlation between stimulus preferences in left posterior middle temporal gyrus and lesion presence.

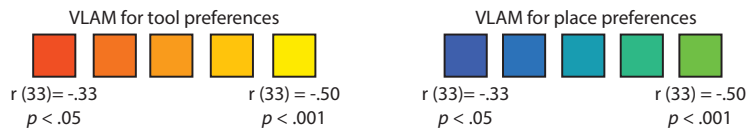
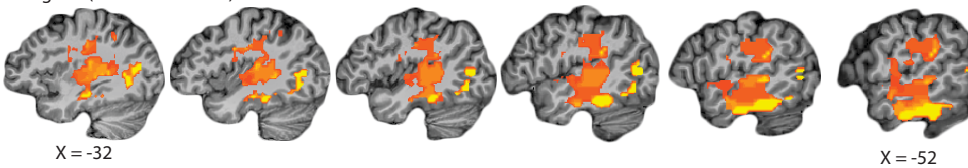
i. Axial (inferior-to-superior)



ii. Coronal (anterior-to-posterior)



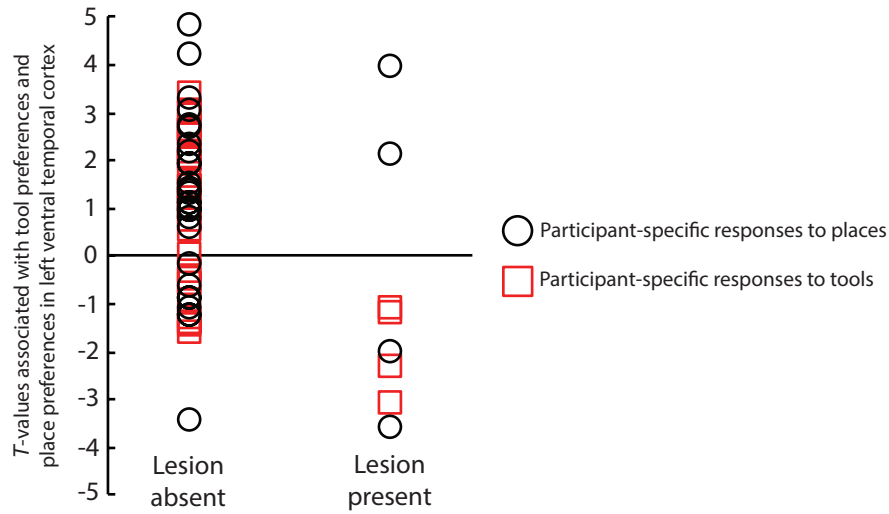
iii. Sagittal (medial-to-lateral)



Supplemental Figure 3. Voxel-based Lesion Activity Mapping (VLAM) showing that lesions to aIPS modulate neural responses to tools in the left posterior middle temporal gyrus.

A. Subject-specific left posterior middle temporal tool-preferring ROIs are represented as spheres (6 mm diameter). Subject-specific tool-preferring ROIs were defined using half of the data (e.g., even runs) from each participant, and the remaining half the data (i.e. odd runs) from that participant were used to calculate category-preferences at the single-subject level (with averaging across the data folds). **B.** Plotted in the bar graphs are contrast-weighted t-values for each category versus the fixation baseline. **C.** Lesions to the left supramarginal gyrus, left anterior intraparietal sulcus, adjacent white matter areas, and the left lateral and anterior temporal lobe are inversely correlated with tool preferences in left ventral temporal cortex (red-to-yellow color-scale). All partial (regressing lesion volume) correlation coefficient values plotted in the map survive cluster correction (cluster correction using AlphaSim, minimum cluster size of 191 voxels, with an initial alpha level of $p < .05$, uncorrected). Note that the VLAM maps are presented in radiological convention.

Supplemental Figure 4. Visualization of participant-specific tool- and place-preferences in left ventral temporal cortex as a function of lesion presence in an example aIPS voxel.



Supplemental Figure 4. Visualization of participant-specific tool- and place-preferences in left ventral temporal cortex as a function of lesion presence in an example aIPS voxel. Visualization of participant-specific tool- and place-preferences in left ventral temporal cortex as a function of lesion presence in an example aIPS voxel. The figure illustrates the dissociation between participant-specific tool (red squares) and place preferences (black circles).

Supplemental Table 1. Demographic information, lesion size, lesion location, and etiology for each neurosurgery patient participant.

Participant	Age	Gender	Lesion Size (1 mm ³ voxels)	Lesion Location	Etiology
1	60	F	14721	Left Frontal-Parietal Cortex	Astrocytoma
2	25	M	75072	Left Inferior Parietal Cortex	Astrocytoma
3	49	F	11193	Left Middle Temporal Gyrus	Glioma
4	34	M	5474	Left Middle Temporal Gyrus	Cerebral Cavernoma
5	43	F	12985	Left Occipital Cortex	Arteriovenous Malformation
6	42	M	48242	Left Frontal-Motor Cortex	Anaplastic Astrocytoma
7	53	M	29325	Right Hippocampus	Anaplastic Astrocytoma
8	48	F	69822	Left Frontal/Pre-motor Cortex	Anaplastic Astrocytoma
9	63	M	103125	Left Frontal/Motor Cortex	Glioblastoma
10	59	M	103966	Left Anterior/Lateral Temporal Lobe	Glioblastoma
11	59	M	67844	Right Anterior Temporal Cortex	Anaplastic Astrocytoma
12	26	M	16759	Right Superior Temporal Sulcus	Astrocytoma
13	66	M	28954	Left Anterior Temporal Lobe	Anaplastic Astrocytoma
14	70	M	15402	Left Hippocampus	Glioma
15	36	F	70914	Left Lateral Temporal/ Inferior Frontal Cortex	Glioma
16	25	F	3383	Left Premotor Cortex	Cavernoma
17	26	M	22334	Left Posterior Parietal Cortex	Complex Partial Epilepsy w/o Status Epilepticus
18	27	M	59126	Right Anterior Temporal Cortex	Complex Partial Epilepsy w/o Status Epilepticus
19	61	F	88604	Right Anterior Temporal/ Frontal Cortex	Glioma
20	36	F	36957	Right Frontal-Motor Cortex	Oligodendroglioma
21	65	M	25987	Right Temporal/Parietal Cortex	Glioma
22	26	M	76946	Right Fronto-Parietal Cortex	Anaplastic Astrocytoma
23	13	F	7540	Left Hippocampus, Amygdala	Glioma
24	55	F	41185	Left Parietal Cortex	Glioblastoma
25	42	M	122614	Left Temporal/Parietal Lesion	Glioblastoma
26	76	M	28576	Left Anterior Temporal Lobe	Glioblastoma
27	34	M	75939	Left Frontal Cortex	Glioma
28	65	F	67194	Right Posterior Parietal Cortex	Glioblastoma
29	28	M	42490	Left Supplementary Motor Area	Oligodendroglioma
30	59	F	15644	Right Motor Cortex	Anaplastic Astrocytoma
31	54	M	63750	Left Posterior Parietal Cortex	Arteriovenous Malformation
32	62	F	22274	Left Frontal/Insular Cortex	Oligodendroglioma
33	46	F	8637	Left Amygdala/ Hippocampal	Glioma
34	57	M	101897	Left Temporal Lobe	Glioblastoma
35	67	M	5520	Left Anterior Intraparietal Sulcus	Glioma